BIODIVERSITAS
Volume 25, Number 11, November 2024
Pages: 4360-4369

ISSN: 1412-033X
E-ISSN: 2085-4722
DOI: 10.13057/biodiv/d251135

Preparation and characterization of chitosan derived from slipper lobster (*Thenus orientalis*)

RAHMAN KARNILA[1,♥], BUSTARI HASAN[1], DIAN IRIANI[1], HARIFA SYAH PUTRA[2], MUHAMMAD FAUZI[3], ZULFARINA[4]

[1]Department of Fisheries Product Technology, Faculty of Fisheries and Marine Science, Universitas Riau. Jl. Kampus Bina Widya Km. 12,5, Pekanbaru 28293, Riau, Indonesia. Tel./fax.: +62-761-63266, ♥email: rahman.karnila@lecturer.unri.ac.id

[2]Department of Marine Science, Faculty of Fisheries and Marine Science, Universitas Riau. Jl. Kampus Bina Widya Km. 12,5, Pekanbaru 28293, Riau, Indonesia

[3]Department of Aquatic Resources Management, Faculty of Fisheries and Marine Science, Universitas Riau. Jl. Kampus Bina Widya Km. 12,5, Pekanbaru 28293, Riau, Indonesia

[4]Department of Education Biology, Faculty of Teacher Training and Education, Universitas Riau. Jl. Kampus Bina Widya Km. 12,5, Pekanbaru 28293, Riau, Indonesia

Manuscript received: 23 August 2024. Revision accepted: 20 November 2024.

Abstract. *Karnila R, Hasan B, Iriani D, Putra HS, Fauzi M, Zulfarina. 2024. Preparation and characterization of chitosan derived from slipper lobster (*Thenus orientalis*). Biodiversitas 25: 4360-4369.* Slipper lobster (*Thenus orientalis* (Lund, 1793)) is a marine fishery commodity that can be utilized its large carapace (proportion >50%) to be converted into chitosan, but ideal, accurate and rapid characterization has not been developed in detecting chitosan and its derivatives as potential raw materials for nutraceuticals. In this study, the proportion and chemical composition of slipper lobster were analyzed, and the carapace of slipper lobster was determined for the degree of deacetylation of chitin and chitosan, then chitosan was evaluated for glycosidic chains using LCMS-MS from ESI sources. The method used was descriptive with 3 repetitions. The results showed that the largest proportion of the slipper lobster body was found in the carapace at 52.98%. The highest mineral content in the carapace is calcium at 752 mg L^{-1} and the lowest is phosphorus at 0.36 mg L^{-1} and higher than meat. The yield value of chitosan was 31.19% with a deacetylation degree of 80.15%. The glycosidic chain of chitosan has many amine groups from the structure of the compound 2-Amino-2-Deoxy-D-Glucose Chitosamine and 2-(Aminomethyl)-N-(3-isopropyl octahydro [1,2,4] triazolo [4,3-a] pyridine-6-il)-1 piperidinekar kotakamida which have high quality chitosan affinity, but there is a compound 5-Aminomethyl-2,4-Dihydro [1,2,4] Triazol-3-One Hydrochloride and N-[3-Methyl-2-(4-methyl-1-piperazinyl)-butyl] isoleucinamide hydrochloride which tends to be dissociated and cationized by HCl. Overall, these data suggest the glycosidic chain of slipper lobster has potential as a raw material for nutraceuticals and functional food ingredients.

Keywords: Chitosan derivatives, deacetylation degree, Liquid Chromatography-Mass Spectrometry (LCMS), slipper lobster

INTRODUCTION

The generation of shrimp squander from the shrimp preparing industry has expanded in later a long time. The persistent generation of these biomaterials without suitable innovation improvement and utilization has come about in squander transfer and contamination issues (Kozma et al. 2024). One of the less well known shrimps with huge carapace (±50%) (Ghorbel-Bellaaj et al. 2011) and potential to contaminate the environment is the shoe lobster. Hence, from both natural and financial viewpoints, fitting advances ought to be connected wherever conceivable to anticipate decay and change over biomaterials into important items such as the arrangement of chitin and chitosan from shrimp carapace.

Chitin is a natural biopolymer usually sourced from crustaceans and contains about 89.59% (Manimohan et al. 2024) and 82.5% from slipper lobster with a deacetylation degree of 65% reported by Mohan et al. (2021). The degree of deacetylation of chitosan greatly affects its application, including biomolecules as carrier substances (Aranaz et al. 2021; Verardi et al. 2023; Mawazi et al. 2024). Therefore, chitosan has unique physicochemical and biological properties such as biocompatibility, biodegradability, bioactivity, low toxicity, mucoadhesion, and structural variability (Jiménez-Gómez and Cecilia 2020; Hameed et al. 2022; Mura et al. 2022). Chitosan's qualities make it applicable in a variety of disciplines, including medical, dental care, food processing chemistry, biotechnology, agriculture, and environmental protection. Furthermore, because of the biopolymer structure of natural polysaccharides, which has many amine groups (NH_2) that are reactive to anionic molecules, it can be used for food raw materials, cosmetics, animal feed antibacterial, textile, and other pharmaceutical products (Arora et al. 2021; Xu et al. 2021a; Tavares et al. 2023; Blasi et al. 2023; Azelee et al. 2023; Zhang et al. 2024). Chitosan as a nutraceutical is strategically important for improving biomolecule stability, bioactivity, and bioavailability (Imam et al. 2021; Xu et al. 2021b; Picos-Corrales et al. 2023). However, high-quality chitin and chitosan must be extracted from the mineralized, proteinaceous sections of the carapace, which is often done using a two-step acid-alkali extraction process including hydrochloric acid and sodium hydroxide (Hisham et al. 2021; Rasweefali et al. 2022). This is because the carapace

contains numerous mineral components like as calcium carbonate, protein, and chitin (Pakizeh et al. 2021).

The source of chitin is a challenge in finding the appropriate conditions for chitin and chitosan extraction because carapace composition differs between crab species (Triunfo et al. 2022). Several attempts to optimize chitin extraction from shrimp, crab, and lobster species have been made (Ghorbel-Bellaaj et al. 2013; Nguyen et al. 2020; Mathaba et al. 2020; Azelee et al. 2023; Manimohan et al. 2024; Zhang et al. 2024), but the literature generally favors the use of randomly selected conditions for decisions on reagent concentration, reagent volume, reaction temperature, and reaction time (Journot et al. 2020; Taylor et al. 2023). This results in extremely high costs and extra chemical waste, particularly when the reaction is scaled up. For these reasons, there is still a lack of detailed information on the optimal circumstances for chitosan structure detection.

Presently, numerous approaches are used to determine the glycosidic structure of chitosan, including titration, elemental, spectroscopic (infrared and ultraviolet), X-ray diffraction, and H NMR studies. Each strategy has its merits and disadvantages. In this context, spectrometry is often used to analyze the degree of deacetylation in chitin and chitosan, but contamination interferes with the ratio and absorption process, resulting in poorer accuracy (Li et al. 2019). The acid-base titration method for determining the degree of deacetylation produces a precipitate, resulting in less accurate results. Furthermore, because of the hydrogel attached to the electrode, the H NMR technique is more sensitive at high deacetylation degree values and takes longer to complete (Zhang et al. 2005). Therefore, the LCMS (Liquid Chromatography-Mass Spectrometry) method is believed to help provide accurate information on the quality of chitosan more specifically by detecting the glycosidic chains in chitosan based on each molecular weight of different compounds. The detection will form negatively and positively charged ions in the ESI source (Xue et al. 2022). LCMS/MS is an effective and quantitative alternative technique for chemical structure analysis (Gosetti et al. 2013; Sivashankari and Prabaharan 2017; Xue et al. 2022). Thus, the chemical composition used can be used as a reference for future research because it obtains accurate data on chitosan profiles (Li et al. 2019; Xue et al. 2022). The review explores slipper lobster chitosan's specific characteristics through glycosidic chain, focusing on biomaterial preparation and potential use for nutraceuticals, despite limited information on its utilization.

MATERIALS AND METHODS

Ingredients and equipments

The primary material used in this study is slipper lobster (*Thenus orientalis* (Lund, 1793)) collected from the waters of Sibolga, North Sumatera, Indonesia. The slipper lobster weighs between 50 and 250 g. The chemicals used for chitin and chitosan include 37% H_2SO_4 (Smart Lab, Indonesian), 1 N HCl (Merck, Germany), 3 N NaOH (Merck, Germany), 30% NaOH, 20% NaOH, methanol (Merck, Germany), 50% acetonitrile (Merck, Germany), DMSO (Merck, Germany), Iodomethane (Merck, Germany). The tools used in this study include vortex, AAS Atomic Absorption Spectrophotometer (Perkin Elmer Analyst 100, USA), Fourier Transform Infra Red (FTIR) spectrophotometer (Shimadzu 21, Japan), centrifuge (eppendorf 5424 R, Germany), magnetic stirrer (velp scientifica, Italy), pH meter, LC-MS (Qtof, Japan), refrigerator (BRP-5V588, China), oven (binder, Germany), incubator (binder, Germany), stopwatch, grinder (EP200, China), analytical scales (0.0000 g) (boeckel, Germany), digital scales (0.00 g) (BC ohaus, Germany), Oasis PRiME HLB column (30 mg/1 cc; Waters, cat. no. 186008055), Erlenmeyer 100 mL, Erlenmeyer 1000 mL, beaker, volumetric pipette, porcelain cup, measuring cup, test tube, hot plate, glass stirrer, tube rack and tray.

Preparation of raw material

Slipper lobster were obtained from fishermen in Sibolga, North Sumatra. A total of 10 kg of slipper lobster measuring 50-250 g/head were sampled and transported on ice to the Aquatic Biology Laboratory, Faculty of Fisheries and Marine Sciences, Pekanbaru. The initial stage, the slipper lobster is separated into carapace, meat, stomach contents, and others. The carapace is washed using running water and brushed to remove the remaining meat attached to the carapace (Putra et al. 2023). The slipper lobster body is weighed before drying the carapace in an oven at 40°C for 5 days. Afterwards, the carapace and meat are ground and analyzed for minerals.

Moisture and ash analysis

Analysis of moisture and ash content was carried out according to AOAC (2007) procedures. Porcelain cups were dried in an oven at 105°C for 2 hours. Then, they were placed in a desiccator for ±15 minutes and weighed, then the samples were crushed using a mortar. As much as 3-4 g into a porcelain cup for the water test and as much as 4-5 g into a porcelain cup for the ash test. For the water test, the samples were placed in an oven at 102-105°C for 5-6 hours. Afterwards, the samples were placed in a desiccator for 15 minutes. Then weighed (repeat this procedure until a fixed weight is obtained). Calculation of moisture content can be done using the formula:

$$\% \text{ Moisture content} = \frac{B - C}{B - A} \text{ x } 100\%$$

Description: A: Porcelain cup weight (g); B: Weight of porcelain cup filled with sample (g); C: Weight of porcelain cup with dried sample (g)

Furthermore, for the ash test, the sample was burned in a furnace at 550°C for 3 hours. Next, the cup was cooled in a desiccator for 30 minutes and weighed. Calculation of ash content can be done using the formula:

$$\% \text{ Ash content} = \frac{C - A}{B - A} \text{ x } 100\%$$

Where: A: Porcelain cup weight (g); B: Weight of cup with sample (g); C: Weight of cup with combustion sample (g)

Mineral analysis

The mineral content of carapace and meat was analyzed for Ca, K, Fe, Na, Mg and P according to AOAC (2007) procedure. Samples were weighed 1-2 g into a 200 mL Erlenmeyer and added 5 mL of 65% nitric acid. Then, heated in a fume hood (deconstruction) for 30 minutes at 200°C. After that, cool and filtered with Whatman paper until the solution is clear. Then, diluted with distilled water to a limit of 80 mL and add 2-3 drops of 50% H_2O_2 solution. The sample and standard solutions were flowed into the Atomic Absorption Spectrophotometer with the wavelength of each mineral type (Ca 422.7 nm; Na 589 nm; K 766.49 nm; Fe 248.3 nm; Mg 400 nm). After the standard absorbance is obtained, it is connected between the standard concentration (as the Y axis) and the standard absorbance (as the X axis) so that a mineral standard curve is obtained with a linear line equation y = ax + b which is used for calculating the concentration of the sample solution. The concentration of the sample solution is calculated by multiplying a by the absorbance (note: y = dependent variable; a = slope/gradient; x = independent variable; and b = constant). The calculation of mineral content (mg L^{-1}) wet basis:

$$\text{Mineral content} = \frac{\text{ppm readable x } f_p}{W} \text{ x } 100\%$$

Where: f_p: Dilution factor; W: Sample weight (g)

Chitin and chitosan extraction

Chitosan extraction refers to Suptijah's (2004) approach, which includes demineralization, deproteinization, and drying before chitosan is produced through chitin deacetylation. The refined shrimp carapace is demineralized with 1N HCl solution (1:7 (w/v)) for 1 hour at ±90°C. The demineralization products are then precipitated by allowing them to stand, separating solids and liquids. The material was rinsed three times with distilled water to neutralize the pH to around 7. The solid was then deproteinized with 3N NaOH solution (ratio of solid to NaOH solution 1:10 (w/v) for 1 hour at a temperature of ±90°C. The results of the deproteinization process were then precipitated to separate the solid and liquid by allowing the solid part to separate from the liquid. The solid obtained was washed repeatedly with tap water to neutralize the pH to near pH 7. The solid was dried in an oven at 60°C for 6 hours. The chitin formed was analyzed for water content, ash, nitrogen and degree of deacetylation. Chitosan was obtained by deacetylating chitin using 30% NaOH solution (ratio of chitin to NaOH solution 1:2 (w/v)) for 1 hour at a temperature of ±100°C. The deacetylation materials were then precipitated to separate the solid and liquid components by allowing the solid to separate from the liquid. The material was rinsed several times with tap water to neutralize the pH to approximately pH 7. The solid was dried in an oven at 60°C for 6 hours. The resulting chitosan was examined for yield (Karnila et al. 2011), degree of deacetylation (Sánchez-Machado et al. 2024), and glycosidic chain (Suzuki 2021).

Measurement of the degree of deacetylation via FTIR

The degree of deacetylation of chitin and chitosan was analyzed using a Fourier Transform Infra Red (FTIR) spectrophotometer from the method of Sánchez-Machado et al. (2024) 2 mg of sample was weighed and 200 mg of KBr was added, then crushed with a mortar. The mixture was pressed with 800 kg pressure using a hydraulic pump tool so that thin pellets were obtained. The pressed pieces were measured for absorbance at wavelengths of 1655 and 3450 cm^{-1}. The highest peak was recorded and measured from the selected baseline. The absorbance value can be measured using the formula:

$$A = log \frac{P_o}{P}$$

Where: A: Absorbance; P: Transmittance at minimum peak; Po: Transmittance at baseline

The degree of deacetylation (DD%) was calculated by comparing the absorbance value at wave number 1655 cm^{-1} (amide band absorption) with wave number 3450 cm^{-1} (hydroxyl band absorption). Undeacetylated chitin and chitosan resulted in a comparison value of A1655/A3450 = 1.33. The degree of deacetylation can be calculated with the following equation:

$$DD\% = 100 - \left[\left(\frac{A_{1655}}{A_{3450}} x \frac{1}{1{,}33}\right)\right]$$

Where: A1655: Absorbance at a wavelength of 1655 cm^{-1}; A3450: Absorbance at a wavelength of 3450 cm^{-1}; 1.33: Constant

The glycosidic chain of chitosan

Based on the molecular weight of the glycosidic chain as determined by LC-MS/MS (Liquid Chromatography Mass Spectrometry) using the ESI (Electrospray Ionization) method, the chitosan chemical content of slipper lobster carapace was calculated, according to the protocol (Suzuki 2021). Using a Hydrophilic-Lipophilic-Balanceid (HLB) mobile phase, samples were produced by Solid Phase Extraction (SPE). The mobile phase was conditioned using methanol solution prior to LCMS readings. Nanocytosan samples, 0.1-0.2 g were crushed in a mortar, 50 µLNaOH/DMSO (super dehydration) was added, and vortexed for 2 min. After that, 15 µL of iodomethane was added and vortexed again for 1 minute and centrifuged at 150 rpm for 1 minute. Then the supernatant was taken and 20 µL of 50% acetonitrile was added and centrifuge 1 min at 150 × g, 25°C. Discard the waste and repeat twice. The sample was inserted in Water's Column Packagec as a syringe containing stationary phase then eluted with methanol. 1-5 µL/injection for in LCMS (flow rate: 0.2 mL/min column oven: 50°C fluorescence detector: Ex: 315 nm, Em: 400 nm) and the resulting chromatogram was then read using the MassLynx V4.1 program to determine the mass spectrum, molecular weight, and molecular formula. The compound names and chemical structures were identified using the Chemspider chemical website.

Analysis data

The research was divided into 3 stages, namely (i) preparation of raw materials and making slipper lobster carapace flour and analyzing the proportion and chemical composition, (ii) extraction of shrimp carapace chitin, chitosan, and analyzing the degree of deacetylation, (iii) chitosan glycosidic chain analyzed using LCMS. Each treatment was repeated 3 times, then analyzed by descriptive analysis and tabulated in the form of figures, tables and graphs using the Statistical for Social Science (SPSS) version 26 program (SPSS, 2022) and MassLynx V4.2.

Characterization of slipper lobster

The slipper lobster (*T. orientalis)* used in this study was a consumption size. The average length of the slipper lobster used ranged from 15.2-24.7 cm. The morphological characteristics of slipper lobster can be seen in Figure 1.

The dorsal slipper lobster is darker, dark brown with a rough skin surface and black spots on the head compared to the ventral position which is lighter, light brown and the body to the tail is pink. The morphology of the slipper lobster body, the head (cephalothorax) is flat and wide (flathead) similar to the shape of a shrimp, flatter, harder and thicker than the body. The body or abdomen is segmented, covered with small, hard spines and covered in lime, then the tail (telson) is upright and has eight legs (Lavalli et al. 2019). Differences between female and male sex in slipper lobster seen that females have larger pleopods, equipped with hairs (setae), larger size, wider abdomen, longer tail and brighter color than male slipper lobster (Holthuis 1985; Kabli and Kagwade 1996; Pratiwi 2011; Kizhakudan 2014; Lavalli et al. 2019). Thus, the unique morphology and physical characteristics of slipper lobster that have been described provide a strong basis for further utilization, as reported by Teoh et al. (2023) that there is L-glutamic acid in slipper lobster (*T. orientalis*) that can be utilized as a functional food. Furthermore, Mergelsberg et al. (2019) reported, there are 7 body parts in lobster (*H. americanus*), namely legs, dominant chela, cephalon, non-dominant chela, thorax, abdomen, and uropods have been investigated, having differences in chemical composition of a good biomineralization process. Therefore, it is necessary to further analyze the great potential in slipper lobster for wider industrial applications.

Components of the body of slipper lobster

The slipper lobster's body consists primarily of flesh, carapace, gonads, and food waste. Meat is a part of the shrimp body that is protected by a thick carapace coating. The gonads are yellow and placed below the abdomen. Food waste is a component of the digestive tract, intestines, and stomach. Figure 2 and Table 1 depict the components of shrimp and their relative proportions.

Overall, the proportion of carapace, meat, gonad and food waste is 13:8:2:1 (w/w). Carapace is the largest part, which covers 52.98% of the total weight of shrimp; followed by meat (35.06%), gonad (7.79%) and food waste (4.17%). Compared with other types of crustaceans, the percentage of carapace of slipper lobster is higher than that of shrimp carapace in general, around 40% (Dai et al. 2023) and crab shells, which is 43.15% (Kraisangsri et al. 2018). Thus, the carapace of slipper lobster is richer in biomass as a source of chitin and chitosan than shrimp and crab. Furthermore, compared to the differences in species (*Thenus indicus* Leach, 1816) and habitat, the slipper lobster in this study were more commercial and had a higher population density of 2.02 ha^{-1} compared to the slipper lobster reported by several researchers, namely 1.78 ha^{-1} (Jones 1993; Modayil et al. 2008).

Table 1. Presentation of body parts of slipper lobster (*T. orientalis*)

Body parts of slipper lobster	Weight (g)	Percentage of weight (%)
Carapace	70.59±19.25	52.98±14.54
Meat	46.72±13.47	35.06±10.17
Gonad	10.38±3.80	7.79±2.94
Food waste	5.56±4.75	4.17±3.59
Total	133.25±41.27	100

Figure 1. Slipper lobster (*Thenus orientalis* (Lund, 1793))

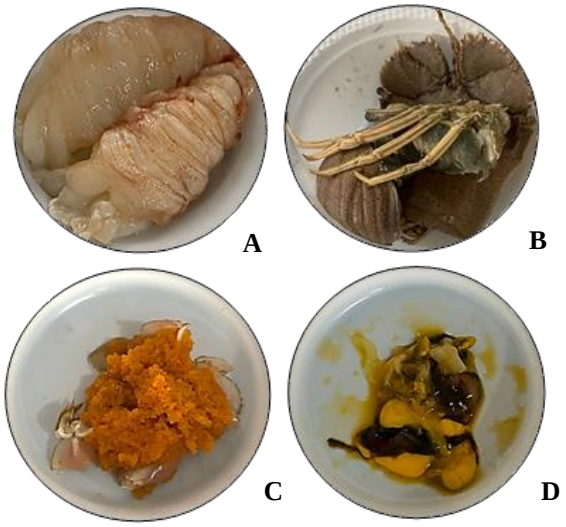

Figure 2. Body parts of slipper lobster. A. Meat; B. Carapace; C. Gonad; D. Leftover food waste

Table 2. Mineral content of carapace and meat of slipper lobster

Content (dry weight)	Carapace	Meat
Moisture (%)	2.26±0.05	-
Ash (%)	53.66±0.06	-
Potassium (mg L^{-1})	55.07±0.14	29.70±0.02
Magnesium (mg L^{-1})	37.12±0.11	0.67±0.52
Calcium (mg L^{-1})	752.34±1.07	0.86±0.01
Sodium (mg L^{-1})	136.82±1.11	7.25±0.27
Iron (mg L^{-1})	12,28±0.20	0.12±0.80
Phosphorus (mg L^{-1})	0.36±0.06	0.004±0.00

Note: (-) not determined

Table 3. Yield of chitin and chitosan of slipper lobster

Component	Yield (%)
Carapace flour	28.71±0.04
Chitin	39.26±2.04
Chitosan	31.19±1.97

A **B**

Figure 3. A. Chitin, B. Chitosan

Chemical content of slipper lobster

Table 2 provides a chemical analysis of the slipper lobster carapace and meat. The chemical composition of carapace was found to be high in calcium (752.34 mg L^{-1}), but flesh was high in potassium (29.70 mg L^{-1}). This calcium level is lower than that of the typical shrimp carapace, which is 61359.70 mg L^{-1} (Al Hoqani et al. 2021), making deacetylation easier during chitosan extraction. The carapace mineral levels in this study were similar to those of slipper lobster reported by Putra et al. (2024) who obtained most of the minerals in the form of the highest calcium, 766.87 mg L^{-1} and Sagheer et al. (2009) reported, a small portion in the form of calcium phosphate (Ca_3PO_4) and the lowest iron (Fe) content of 2.44 mg L^{-1}. Therefore, the mineral content of the carapace is higher than that of the meat, which indicates the large amount of minerals formed in the carapace, such as Ca, K, Na, Mg, Fe and P (Sagheer et al. 2009; Ghorbel-Bellaaj et al. 2011; Rasti et al. 2017; Arasukumar et al. 2019). The reason is also proven by the high ash content of 53.66% (Table 2). Another reason is supported by Pakizeh et al. (2021) that shrimp carapace contains three main components, namely 15-40% α-chitin, 20-40% protein, and 20-50% CaCO3.

Yield of chitin and chitosan

The percentage of chitin and chitosan extracted from carapace flour is referred to as yield. Table 3 shown in the percentage yield of carapace flour, chitin, and chitosan. The yields of chitin and chitosan were 39.26% and 31.19% respectively. Chitin yield in this study was relatively high from slipper lobster, namely 17.50%, small crab, namely 21.25% (Mohan et al. 2021), *Panaeus monodon* Fabricius, 1798 shrimp, namely 30% (Srinivasan et al. 2018), *Thenus unimaculatus* Burton & Davie, 2007, namely 35% (Arasukumar et al. 2019), sand sea cucumber, namely 20.13% (Sumarto et al. 2020) and fish scales, namely 31.11% (Alabaraoye et al. 2017). Furthermore, the chitosan yield in this study was also relatively high compared to the type of crab, namely 20.64% (Syukron et al. 2016), butterfly shrimp, namely 27.51% (Ghazali 2019), Vanname shrimp, namely 19.5% (Yuliasara 2019), and tiger shrimp, namely 14% (Cahyono 2018). The yield of chitin and chitosan in fishery products is greatly determined by the type of material, the amount of mineral content and protein hydrolyzed by acids and bases.

Physical characteristics of chitin and chitosan

Dried and ground shrimp carapace was extracted through deproteination and demineralization processes to produce chitin, and then deacetylated (-CH_3CO) to produce chitosan. The characteristics of chitin and chitosan are shown in Figure 3.

Chitin and chitosan are light brown in color, with a smoother texture, slightly lumpy, and odorless. These changes are caused by demineralization, deproteinization, and deacetylation processes with HCl and NaOH, which result in a condensation reaction that hydrolyzes the N-acetylglucosamine monomer, making chitin and chitosan smoother, whiter, and odorless (Zhang et al. 2021). The color properties of chitin and chitosan in this study fulfilled the criteria, ranging from light brown to white (SNI 7948 and 7949: 2013).

Degree of deacetylation of chitin and chitosan

The degree of deacetylation of chitin was 60.56% and chitosan was 80.15%. In this study, the degree of deacetylation of chitin was lower than that of slipper lobster which was 65%, mantis shrimp 68%, and swimming crab 70% (Mohan et al. 2021). This difference is thought to be due to the high ash and mineral content in chitin as a result of not being released during the demineralization process. This reason is also proven by the relatively low degree of deacetylation of chitin from the SNI standard, which is >65% (SNI 7948: 2013). The degree of deacetylation of chitosan in this study meets the SNI standard, which is >75% (SNI 7949: 2013). The degree of deacetylation of chitosan is higher than that of mantis shrimp 78.04% (Putra et al. 2023), blue crab 71.03% (Syukron et al. 2016), mangrove crab 52.63% (Karnila et al. 2021), sand sea cucumber 76.83% (Sumarto 2020) and shrimp as general 76.46% (William and Wid 2019), but lower than tiger shrimp 98.65% (Cahyono 2018) and freshwater lobster around 92.06% (Kadak et al. 2023). The higher the degree of deacetylation causes the free

electron pair (cation) in the amine group to be more reactive (Boroumand et al. 2021). The difference in the degree of deacetylation also depends on the material, acid-base concentration, soaking time and extraction method used.

Chitosan glycosidic chain

The findings of LC-MS QTOF analysis of the glycosidic chain of chitosan with a deacetylation degree of 80.15% yielded four dominating chromatogram peaks (Figure 4), with an accuracy of more than 90%. Table 4 shows the chemicals found using Masslynx analysis. In this study, the glycosidic chain of chitosan tends to dissociate at mass spectra of 150 m/z with molecular ion $[C_3H_7ClN_4O^+H]^+$, 156 m/z with molecular ion $[C_6H_{13}NO_5{}^+H]^+$, 330 m/z with molecular ion $[C_{16}H_{33}ClN_6O^+H]^+$, and 760 m/z with molecular ion $[C_{16}H_{33}N_6{}^+H]^+$. The $C_6H_{13}NO_5$ molecule detected the chemical 2-Amino-2-Deoxy-D-Glucose Chitosamine, also known as Glucosamine (Figure 4.B). This compound has a molecular weight of 179.171 Da with a fragmentation pattern close to the high-quality chitosan (162.08 Da) reported by Abdulsahib et al. (2016), Li et al. (2019) and Xue et al. (2022). However, it has not met the standard of commercial chitosan (Sigma-Aldrich) with a molecular weight of 50-130 Da (Alisson 2020). Nonetheless, chitosan has different copolymers after detection by ESI. This glucosamine compound is the main component of chitosan from monomeric units with glycosidic bonds that form complex polymers (Gonçalves et al. 2021; Piekarska et al. 2023). This compound has been utilized as a health product because it has biochemical and physiological effects on the body and has been shown to inhibit the production of pro-inflammatory cytokines in inflammation in the body and connective tissue through increasing collagen (Thebiotek 2024). In addition, the producer of glycosaminoglycan chains that form proteoglycans in the body to produce synovial fluid against osteoarthritis disease (Karnila et al. 2021; Sumarto 2020), antibacterial decay and pathogens, anti-inflammatory, nanocarrier, antioxidant, and cholesterol lowering and other functional properties that can reduce intracellular hydroxyl radicals (reactive oxygen species) (Stefaniak et al. 2022; Zhi-Hou et al. 2020; Zhou et al. 2022; Priyanka et al. 2022; Li et al. 2023; Karnila et al. 2023).

Furthermore, the increased intensity of the mass spectra in this study indicates the glycosidic bond tends to be disrupted by other compounds in the ESI source. This is also evidenced by the presence of $C_3H_7ClN_4O+H$ and $C_{16}H_{33}ClN_6O+H$ ions that are still cationized by HCl (Figures 4.A and 4.C). As reported by Li et al. (2019) that the process of glycosidic chain breaking using HCl may be detected in the ESI source. However, the glycosidic bonds bound by such compounds (chitooligomers) from chitin and chitosan production usually have interesting bioactivity properties in medicinal and agricultural systems without affecting their functional properties (Zhang et al. 2015). Kumirska et al. (2010) reported chitosan derivatives detected by LC-MS through a combination of Quadrupole and Time-of-Flight (Q-TOF), very easy to detect ions (positive and negative ions, electrospray ionization, scanning) and usually protonated $[M+H]^+$ and $[M+Na]^+$. Therefore, the chitosan derivatives in this study were bound by negative ions from HCl. In this study, the molecule $C_3H_7ClN_4O$ detected which is still cationized has physiological functions. It is used in pharmacological applications to synthesize various heterocyclic compounds, peptides, peptidomimetics. These compounds can interact with protein molecules and nucleic acids in biological systems such as cell culture. Various in vitro and in vivo studies have shown that these compounds can affect gene expression and enzyme activity, as well as cell metabolism with antioxidative and antiapoptotic compounds BenchChem (2024), Aboelnaga et al. (2017) dan (Thebiotek 2024) reported that $C_3H_7ClN_4O$ has the most powerful biological activity ability in inhibiting cancer cell growth and antibacterial through the mechanism of inhibiting DNA synthesis and cell division by inducing apoptosis or programmed cell death specifically in breast, lung and colon cancer.

Table 4. The existence of chitosan compounds from slipper lobster through glycosidic chains

Compounds	Molecular formula	Average mass (Da)	Monoisotopic mass (Da)	Retention time*
5-Aminomethyl-2,4-dihydro [1,2,4] triazol-3-one hydrochloride	$C_3H_7ClN_4O$	150.567	150.031	1.15[a]
2-Amino-2-deoxy-D-glucose chitosamine	$C_6H_{13}NO_5$	179.171	179.079	4,55[b]
N-[3-Methyl-2-(4-methyl-1-piperazinyl)-butyl] isoleucinamide hydrochloride	$C_{16}H_{33}ClN_6O$	334.928	334.250	7.38[c]
2-(aminometil)-N-(3-isopropil oktahidro [1,2,4] triazolo [4,3-a] piridin-6-il)-1 piperidinekar kotakamida	$C_{16}H_{33}N_6O$	758.926	758.570	15.23[d]

Note: * The chromatograms are shown in Figure 4; [a] Retention time shows chromatogram A; [b] Retention time shows chromatogram B; [c] Retention time shows chromatogram C; [d] Retention time shows chromatogram D

This molecule shares similar functional properties with the $C_{16}H_{33}N_6O$ molecule detected in the compound 2-(Aminomethyl)-N-(3-isopropyl octahydro [1,2,4] triazolo [4,3-a] pyridine-6-il)-1-piperidinekar kotakamida (Figures 4.C and 4.D). These compounds belong to one of the 1,2,4 triazole derivatives that possess significant biological properties including antimicrobial, antiviral, antitubercular, anticancer, anticonvulsant, analgesic, antioxidant, antifungal, anticoagulant, antitubercular, antidiabetic, anti-inflammatory, antihyperlipidemic, anticancer and antidepressant activities (Hernández-Gil et al. 2013; Kumar et al. 2021; Matin et al. 2022). Varum et al. (1991) have studied the chemical structure and presence of N-acetylglucosamine of chitosan (prepared under homogeneous and heterogeneous conditions) showing the degree of deacetylation, amino groups $N(CH_3)_2$ and $N(CH_3)_3$ from NMR spectroscopy on commercial chitosan. From the results of this study, proton and carbon shifts occurred indicating that the presence of triazole indicates deacetylation of chitosan. These inherent properties of triazole compounds have become key chromophores with immense medicinal value and attracted scientists including chemical, agricultural, supramolecular, pharmaceutical, polymer and materials sciences (Chang et al. 2011; Aggarwal et al. 2020; Kumar et al. 2021; Strzelecka and Świątek 2021).

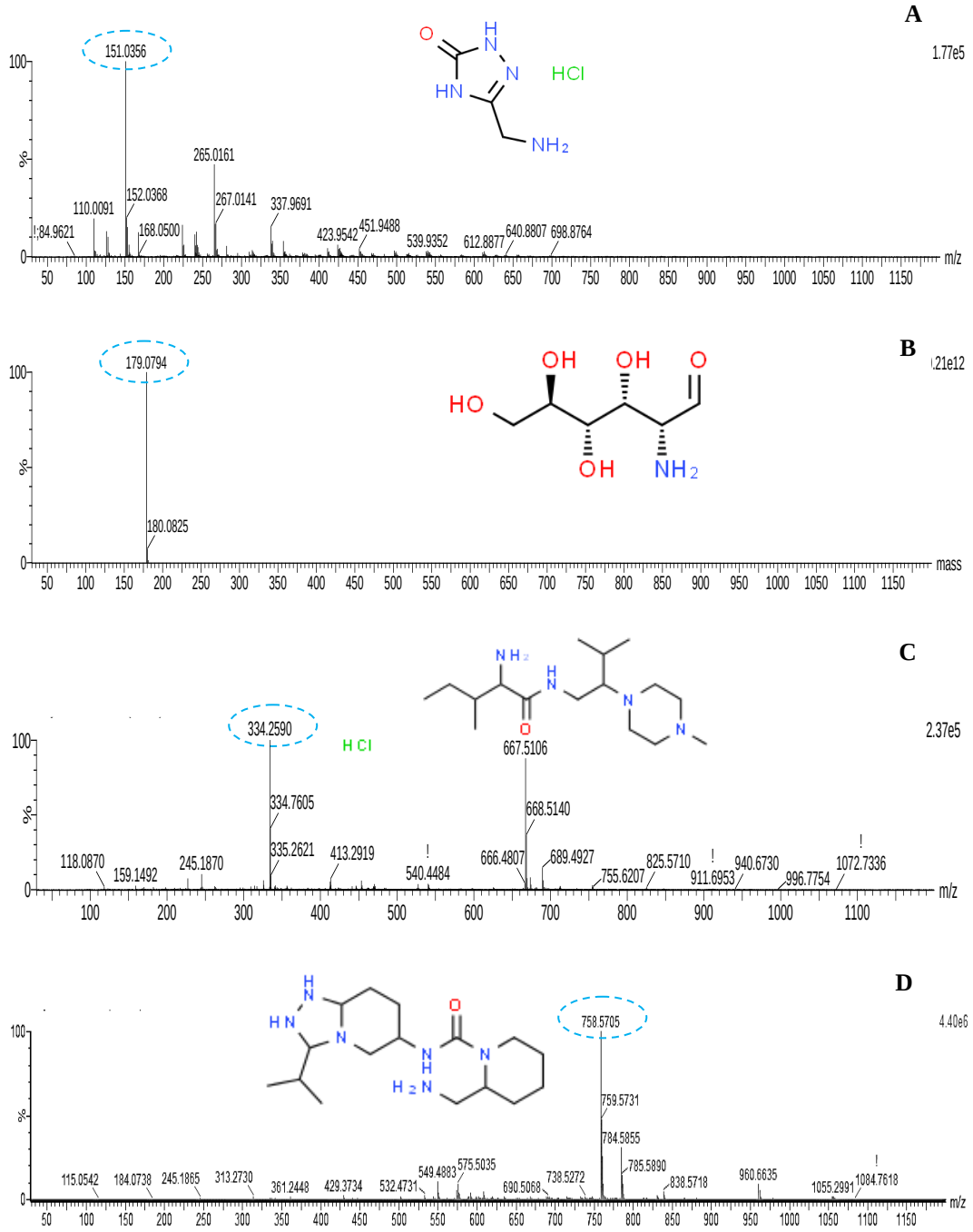

Figure 4. Chitosan chromatogram of slipper lobster using LCMS QTOF

Moreover, the molecule $C_{16}H_{33}ClN_6O$ in this study detected the compound N-[3-Methyl-2-(4-methyl-1-piperazinyl)-butyl] isoleucinamide hydrochloride which has a chain that forms a piperazine group, consisting of two nitrogen rings connected by two carbon atoms, and a ring structure with two nitrogen atoms in the molecule (Lin et al. 2012). The formation of a methyl group, consisting of three carbon atoms and eight hydrogen atoms bonded to one carbon atom. The combination of piperazine groups and methyl groups can be found in various organic compounds for pharmaceuticals (Kilbile et al. 2023). Other compounds containing piperazine groups and methyl groups also have functional properties, namely methisoprinol and N-N'-dimethylpiperazine which are used as atypical antipsychotic drugs (Mauri et al. 2014) and sulfonylpiperazines which have potential as antidiabetic, antibacterial, antifungal, anti-TB, anti-inflammatory, antioxidant and anticancer (Kilbile et al. 2023).

The overall glycosidic chain is similar to high-quality chitosan due to the dissociation process at mass spectra of 341, 381, 484.22, 747, and 806.33 m/z (Li et al. 2019; Alisson 2020). This demonstrates that the chitosan has an accurate dissociation efficiency. However, it was not discovered beyond 1000 m/z, most likely because the chitosan was not detected and the chain is less stable, causing damage to oligomers. Some chitosan structures were found to be changed by the length of time, temperature, and concentration of acid and base immersion, but they retained physiological and biological health potential. FDA (2017) added that to improve the quality and purity of chitosan as a nutraceuticals product, it is necessary to conduct (i) in vivo subject testing in the collection of efficacy, toxicity, pharmacokinetics (preclinical); (ii) oral bioavailability and drug half-life; (iii) dose range for safety; (iv) drug testing in humans to assess side effects; (v) post-marketing surveillance.

In conclusion, slipper lobster carapace has greater biomass of 52.98% and yield of 31.19% with deacetylation degree of 80.15% so that it can be utilized as chitosan biomaterial for large-scale production. The glycosidic chain of chitosan tends to dissociate and detected compounds 5-Aminomethyl-2,4-Dihydro[1,2,4]Triazol-3-One Hydrochloride and N-[3-Methyl-2-(4-methyl-1-piperazinyl)-butyl]isoleucinamide hydrochloride cationized by HCl. In contrast to the compounds 2-Amino-2-Deoxy-D-Glucose Chitosamine and 2-(Aminomethyl)-N-(3-isopropyl octahydro [1,2,4] triazolo [4,3-a] pyridine-6-il)-1 piperidinekar kotakamida which have high quality chitosan proximity. This compound is proven to have potential for nutraceuticals raw materials. However, the sensitivity of the degree of deacetylation needs to be improved through a more optimized chitosan extraction process because the mass spectrum did not detect more than 1000 m/z which is potentially damaged.

ACKNOWLEDGEMENTS

The authors would like to thank DIPA UNRI in 2024 for the funds provided in this research. This study wash conducted within the framework of the project No. 937/UN19.5.1.3/AL.04/2024 funded by DIPA for reaserch and community service, Universitas Riau 2024.

REFERENCES

Abdulsahib HT, Taobi AH, Hashem SS. 2016. A novel coagulant based on chitosan and lignin for the removal of bentonite from raw water. Adv J Sci Res 1 (1): 1-10.

Aboelnaga A, Sahar S, Mohamed H. 2017. A novel chitosan 3-amino-1,2,4-triazole hybrid: Preparation and its effects on cotton fabric properties. J Taibah Univ Sci 11 (5): 768-774. DOI: 10.1016/j.jtusci.2016.08.008.

Aggarwal R, Sumran G. 2020. An insight on medicinal attributes of 1,2,4-triazoles. Eur J Med Chem 205: 112652. DOI: 10.1016/j.ejmech.2020.112652.

Alabaraoye E, Achilonu M, Hester R. 2017. Biopolymer (Chitin) from various marine seashell waste: Isolation and characterization. J Polym Environ 26: 2207-2218. DOI: 10.1007/s10924-017-1118-y.

Alisson CL. 2020. Development of LC-MS And degradation techniques for the analysis of fungal-derived chitin. [Dissertation]. Colorado State University, Colorado. [Amerika Serikat]

Al Hoqani HA, Al Shaqsi NH, Hossin MA, Al Sibani MA. 2021. Structural characterization of polymeric chitosan and mineral from Omani shrimp shells. Water-Energy Nexus 4: 199-207. DOI: 10.1016/j.wen.2021.11.002.

Al Sagheer FA, Al-Sughayer MA, Muslim S, Elsabee MZ. 2009. Extraction and characterization of chitin and chitosan from marine sources in Arabian Gulf. Carbohydr Polym 77 (2): 410-419. DOI: 10.1016/j.carbpol.2009.01.032.

Aranaz I, Alcántara AR, Civera MC, Arias C, Elorza B, Caballero AH, Acosta N. 2021. Chitosan: An overview of its properties and applications. Polymers (Basel) 13 (19): 3256. DOI: 10.3390/polym13193256.

Arasukumar B, Prabakaran G, Gunalan B, Moovendhan M. 2019. Chemical composition, structural features, surface morphology and bioactivities of chitosan derivatives from lobster (*Thenus unimaculatus*) shells. Intl J Biol Macromol 135: 1237-1245. DOI: 10.1016/j.ijbiomac.2019.06.033.

Arora K, Kumar P, Bose D, Li X, Kulshrestha S. 2021. Potential applications of algae in biochemical and bioenergy sector. 3 Biotech 11 (6): 296. DOI: 10.1007/s13205-021-02825-5.

AOAC (Association of Official Analytical Chemists). 2007. Official Methods of Analysis of AOAC International. 18th Edition. AOAC International, Gaithersburg.

Azelee NIW, Dahiya D, Ayothiraman S, Noor NM, Rasid ZIA, Ramli ANM, Ravindran B, Iwuchukwu FU, Selvasembian R. 2023. Sustainable valorization approaches on crustacean wastes for the extraction of chitin, bioactive compounds and their applications - A review. Intl J Biol Macromol 253 (Pt 2): 126492. DOI: 10.1016/j.ijbiomac.2023.126492.

BenchChem. 2024. Manufacturer and supplier of high quality specialty chemicals. Department RnD, US. https://www.benchchem.com. [Accessed Agust 9, 2024]

Blasi A, Verardi A, Lopresto CG, Siciliano S, Sangiorgio P. 2023. Lignocellulosic agricultural waste valorization to obtain valuable products: An overview. Recycling 8 (4): 61. DOI: 10.3390/recycling8040061.

Boroumand H, Badie F, Mazaheri S, Seyedi ZS, Nahand JS, Nejati M, Baghi HB, Abbasi-Kolli M, Badehnoosh B, Ghandali M, Hamblin MR, Mirzaei H. 2021. Chitosan-based nanoparticles against viral infections. Front Cell Infect Microbiol 11: 643953. DOI: 10.3389/fcimb.2021.643953.

Cahyono. 2018. Characteristics of chitosan from tiger shrimp shell waste (*Panaeus monodon*). Jurnal Akuatika Indonesia 3 (2): 96-102. [Indonesian]

Chang JJ, Wang Y, Zhang HZ, Zhou CH, Geng RX, Ji Q. 2011. Recent advances in researches of triazole-based supramolecular chemistry and medicinal drugs. Chem J Chin Univ 32 (9): 1970-1985. [Chinese]

Dai J, Tian S, Yang X, Liu Z. 2023. Synthesis methods of 1,2,3-/1,2,4-triazoles: A review. Front Chem 10: 891484. DOI: 10.3389/fchem.2022.891484.

Dai P, Li D, Sui J, Kong J, Meng X, Luan S. 2023. Prediction of meat yield in the Pacific whiteleg shrimp *Penaeus vannamei*. Aquaculture 577: 739914. DOI: 10.1016/j.aquaculture.2023.739914.

Food and Drug Administration (FDA). 2017. Authority Over Cosmetics: How Cosmetics Are Not FDA- Approved, but Are FDA-Regulated. US. https://www.fda.com. [Accessed August 12 2024]

Ghazali TM, Rahman K, Dewita. 2019. Characteristics and effectiveness of chitosan orininated from the carapace of *T. anomala* shrimp as an antibacterial compound. Berkala Perikanan Terubuk 47 (1): 93-101. DOI: 10.31258/terubuk.47.1.93-101.

Ghorbel-Bellaaj O, Noomen H, Kemel J, Islem Y, Hana M, Ridha H, Moncef N. 2011. Shrimp waste fermentation with *Pseudomonas aeruginosa* A2: Optimization of chitin extraction conditions through Plackett-Burman and response surface methodology approaches. Intl J Biol Macromol 48 (4): 596-602. DOI: 10.1016/j.ijbiomac.2011.01.024.

Ghorbel-Bellaaj O, Hajji S, Younes I, Chaabouni M, Nasri M, Jellouli K. 2013. Optimization of chitin extraction from shrimp waste with Bacillus pumilus A1 using response surface methodology. Intl J Biol Macromol 61: 243-250. DOI: 10.1016/j.ijbiomac.2013.07.001.

Gonçalves C, Ferreira N, Lourenço L. 2021. Production of low molecular weight chitosan and Chitooligosaccharides (COS): A Review. Polymers (Basel) 13 (15): 2466. DOI: 10.3390/polym13152466.

Gosetti F, Mazzucco E, Gennaro MC, Marengo E. 2013. Ultra high performance liquid chromatography tandem mass spectrometry determination and profiling of prohibited steroids in human biological matrices. A review. J Chromatogr B Anal Technol Biomed Life Sci 927: 22-36. DOI: 10.1016/j.jchromb.2012.12.003.

Hameed AZ, Raj SA, Kandasamy J, Baghdadi MA, Shahzad MA. 2022. Chitosan: A sustainable material for multifarious applications. Polymers (Basel) 14 (12): 2335. DOI: 10.3390/polym14122335.

Hernández-Gil J, Ferrer S, Ballesteros R, Castiñeiras A. 2013. N-(5-Amino-1H-1,2,4-triazol-3-yl) pyridine-2-carboxamide. Acta Crystallogr Sect E Struct Rep Online 69 (Pt 2): o227-8. DOI: 10.1107/S1600536813000123.

Hisham F, Akmal MM, Ahmad FB, Ahmad K. 2021. Facile extraction of chitin and chitosan from shrimp shell. Mater Today: Proc 42 (5): 2369-2373. DOI: 10.1016/j.matpr.2020.12.329.

Holthuis LB. 1985. A revision of the family Scyllaridae (Crustacea Decapoda Macrura). I. Subfamily Ibacinae. Zool Verh 218: 1-130.

Imam SS, Alshehri S, Ghoneim MM, Zafar A, Alsaidan OA, Alruwaili NK, Gilani SJ, Rizwanullah M. 2021. Recent advancement in chitosan-based nanoparticles for improved oral bioavailability and bioactivity of phytochemicals: Challenges and perspectives. Polymers (Basel) 13 (22): 4036. DOI: 10.3390/polym13224036.

Jiménez-Gómez CP, Cecilia JA. 2020. Chitosan: A natural biopolymer with a wide and varied range of applications. Molecules 25 (17): 3981. DOI: 10.3390/molecules25173981.

Jones CM. 1993. Population structure of *Thenus orientalis* and *T. indicus* (Decapoda: *Scyllaridae*) in northeastern Australia. Mar Ecol Prog Ser 97: 143-155.

Journot CMA, Nicolle L, Lavanchy Y, Gerber-Lemaire S. 2020. Selection of water-soluble chitosan by microwave-assisted degradation and pH-controlled precipitation. Polymers (Basel) 12 (6): 1274. DOI: 10.3390/polym12061274.

Kabli LM, Kagwade PV. 1996. Morphometry and conversion factors in the sand lobster *Thenus orientalis* (Lund) from Bombay Waters. Indian J Fish 43 (3): 149-254.

Kadak AE, Küçükgülmez A, Çelik M. 2023. Preparation and characterization of crayfish (*Astacus leptodactylus*) chitosan with different deacetylation degrees. Iran J Biotechnol 21 (2): e3253. DOI: 10.30498/ijb.2023.323958.3253.

Karnila R, Dewita E, Yoswatyy D, Putri T, Yunus A. 2023. Antioxidant activity on protein hydrolysate peptide of mudskipper fish (*Periophthalmodon schlosseri*) using alcalase enzyme. Food Sci Technol 43: 1-8. DOI: 10.5327/fst.122222.

Karnila R, Loekman S, Humairah S. 2021. The use of different deacetylation temperature toward quality of chitosan mud crab shell (*Scylla serrata*). IOP Conf Ser: Earth Environ Sci 934: 012092. DOI: 10.1088/1755-1315/934/1/012092

Karnila R, Astawan M, Sukarno, Wresdiyati T. 2011. Nutrient content analysis of fresh sand cucumber meat and flour. Berkala Perikanan Terubuk 39 (2): 51-52. [Indonesian]

Kilbile JT, Tamboli Y, Gadekar SS, Islam I, Supuran CT, Sapkal SB. 2023. An insight into the biological activity and structure-based drug design attributes of sulfonylpiperazine derivatives. J Mol Struct 1278: 134971. DOI: 10.1016/j.molstruc.2023.134971.

Kizhakudan JK. 2014. Reproductive biology of the female shovel-nosed lobster *Thenus unimaculatus* (Burton and Davie, 2007) from north-west coast of India. Indian J Mar Sci 43 (6): 927-935.

Kozma M, Acharya B, Bissessur R. 2022. Chitin, chitosan, and nanochitin: Extraction, synthesis, and applications. Polymers (Basel) 14 (19): 3989. DOI: 10.3390/polym14193989.

Kraisangsri J, Nalinanon S, Riebroy S, Yarnpakdee S, Ganesan P. 2018. Physicochemical characteristics of glucosamine from blue swimming crab (*Portunus pelagicus*) shell prepared by acid hydrolysis. Walailak J Sci Technol 15 (12): 869-877. DOI: 10.48048/wjst.2018.3666.

Kumar S, Khokra SL, Yadav A. 2021. Triazole analogues as potential pharmacological agents: A brief review. Future J Pharm Sci 7: 106. DOI: 10.1186/s43094-021-00241-3.

Kumirska J, Czerwicka M, Kaczyński Z, Bychowska A, Brzozowski K, Thöming J, Stepnowski P. 2010. Application of spectroscopic methods for structural analysis of chitin and chitosan. Mar Drugs 8 (5): 1567-1636. DOI: 10.3390/md8051567.

Lavalli K, Spanier E, Goldstein J. 2019. Scyllarid Lobster Biology and Ecology. IntechOpen. DOI: 10.5772/intechopen.88218.

Li FX, Zhao HY, Lin TF, Jiang YW, Liu D, Wei C, Zhao ZY, Yang ZY, Sha F, Yang ZR, Tang JL. 2023. Regular glucosamine use may have different roles in the risk of site-specific cancers: Findings from a large prospective cohort. Cancer Epidemiol Biomark Prev 32 (4): 531-541. DOI: 10.1158/1055-9965.EPI-22-1134.

Li J, Chen L, Meng Z, Dou G. 2019. Development of a mass spectrometry method for the characterization of a series of chitosan. Intl J Biol Macromol 121: 89-96. DOI: 10.1016/j.ijbiomac.2018.09.194.

Lin HH, Zheng XL, Cao SL. 2012. 5-Methyl-3,3-bis-(4-methyl-piperazin-1-yl)-1-[2-(4-methyl-piperazin-1-yl)eth-yl]indolin-2-one. Acta Crystallogr Sect E Struct Rep Online 68 (Pt 6): o1855. DOI: 10.1107/S1600536812022416.

Manimohan M, Rahaman M, Pandiaraj S, Thiruvengadam M, Pugalmani S. 2024. Exploring biological activity and in-vitro anticancer effects of a new biomaterial derived from Schiff base isolated from *Homarus americanus* (Lobster) shell waste. Sustain Chem Pharm 37: 101363. DOI: 10.1016/j.scp.2023.101363.

Mathaba M, Daramola MO. 2020. Effect of chitosan's degree of deacetylation on the performance of PES membrane infused with chitosan during AMD treatment. Membranes (Basel) 10 (3): 52. DOI: 10.3390/membranes10030052.

Matin MM, Matin P, Rahman MR, Ben Hadda T, Almalki FA, Mahmud S, Ghoneim MM, Alruwaily M, Alshehri S. 2022. Triazoles and their derivatives: Chemistry, synthesis, and therapeutic applications. Front Mol Biosci 9: 864286. DOI: 10.3389/fmolb.2022.864286.

Mauri MC, Paletta S, Maffini M, Colasanti A, Dragogna F, Di Pace C, Altamura AC. 2014. Clinical pharmacology of atypical antipsychotics: An update. EXCLI J 13: 1163-1191. DOI: 10.17877/DE290R-7037.

Mawazi SM, Kumar M, Ahmad N, Ge Y, Mahmood S. 2024. Recent applications of chitosan and its derivatives in antibacterial, anticancer, wound healing, and tissue engineering fields. Polymers (Basel) 16 (10): 1351. DOI: 10.3390/polym16101351.

Mergelsberg ST, Ulrich RN, Xiao S, Dove PM. 2019. Composition systematics in the exoskeleton of the American Lobster, *Homarus americanus* and implications for Malacostraca. Front Earth Sci 7: 69. DOI: 10.3389/feart.2019.00069.

Modayil MJ, Sathiadhas R, Gopakumar G. 2008. India. In: Lovatelli A, Phillips MJ, Arthur JR, Yamamoto K (eds.). FAO/NACA regional workshop on the future of mariculture: A regional approach for responsible development in the Asia-Pacific Region. Guangzhou, China, 7-11 March 2006.

Mohan K, Muralisankar T, Jayakumar R, Rajeevgandhi C. 2021. A study on structural comparisons of a-chitin extracted from marine crustacean shell waste. Carbohydr Polym Technol Appl 2: 100037. DOI: 10.1016/j.carpta.2021.100037.

Mura P, Maestrelli F, Cirri M, Mennini N. 2022. Multiple roles of chitosan in mucosal drug delivery: An updated review. Mar Drugs 20 (5): 335. DOI: 10.3390/md20050335.

Nguyen TT, Luo X, Su P, Balakrishnan B, Zhang W. 2020. Highly efficient recovery of nutritional proteins from Australian Rock lobster heads (*Jasus edwardsii*) by integrating ultrasonic extraction and chitosan co-precipitation. Innov Food Sci Emerg Technol 60: 102308. DOI: 10.1016/j.ifset.2020.102308.

Pakizeh M, Moradi A, Ghassemi T. 2021. Chemical extraction and modification of chitin and chitosan from shrimp shells. Eur Polym J 159: 110709. DOI: 10.1016/j.eurpolymj.2021.110709.

Picos-Corrales LA, Morales-Burgos AM, Ruelas-Leyva JP, Crini G, García-Armenta E, Jimenez-Lam SA, Ayón-Reyna LE, Rocha-Alonzo F, Calderón-Zamora L, Osuna-Martínez U, Calderón-Castro A, De-Paz-Arroyo G, Inzunza-Camacho LN. 2023. Chitosan as an outstanding polysaccharide improving health-commodities of humans and environmental protection. Polymers (Basel) 15 (3): 526. DOI: 10.3390/polym15030526.

Piekarska K, Sikora M, Owczarek M, Jóźwik-Pruska J, Wiśniewska-Wrona M. 2023. Chitin and chitosan as polymers of the future-obtaining, modification, life cycle assessment and main directions of application. Polymers (Basel) 15 (4): 793. DOI: 10.3390/polym15040793.

Pratiwi R. 2011. Sand shrimp (*Thenus* spp.) which is not widely known. Oseanografi-LIPI Vol XXXVI (2): 41-48. [Indonesian]

Priyanka DN, Prashanth KH, Tharanathan RN. 2022. A review on potential anti-diabetic mechanisms of chitosan and its derivatives. Carbohydr Polym Technol Appl 3: 100188. DOI: 10.1016/j.carpta.2022.100188.

Putra MR, Karnila R, Hasan B. 2023. Potential chitosan of waste shell mantis shrimp (*Harpiosquilla raphidea*) as antibacterial. Asian J Aquat Sci 6 (1): 129-135. DOI: 10.31258/ajoas.6.1.129-135.

Putra HS, Hasan B, Karnila R, Ghazali TM. 2024. Mineral content profile of carapace flour, chitin, and chitosan slipper lobster (*Thenus orientalis*). Asian J Aquat Sci 7 (2): 192-199. DOI: 10.31258/ajoas.7.2.192-199.

Rasti H, Parivar K, Baharara J, Iranshahi M, Namvar F. 2017. Chitin from the mollusc chiton: Extraction, characterization and chitosan preparation. Iran J Pharm Res 16 (1): 366-379.

Rasweefali MK, Sabu S, Azad KM, Rahman MR, Sunooj KV, Sasidharan A, Anoop KK. 2022. Influence of deproteinization and demineralization process sequences on the physicochemical and structural characteristics of chitin isolated from Deep-sea mud shrimp (*Solenocera hextii*). Adv Biomark Sci Technol 4: 12-27. DOI: 10.1016/j.abst.2022.03.001.

Sánchez-Machado DI, López-Cervantes J, Escárcega-Galaz AA, Campas-Baypoli ON, Martínez-Ibarra DM, Rascón-León S. 2024. Measurement of the degree of deacetylation in chitosan films by FTIR, ^{1}H NMR and UV spectrophotometry. MethodsX 12: 102583. DOI: 10.1016/j.mex.2024.102583.

Sivashankari PR, Prabaharan M. 2017. Deacetylation modification techniques of chitin and chitosan. In: Jennings JA, Bumgardner JD (eds.). Chitosan Based Biomaterials 1. Woodhead Publishing, Cambridge, UK.

Statistical Package for the Social Sciences (SPSS). 2022. IBM SPSS software. US. https://www.ibm.com/id-id/spss.

Srinivasan H, Kanayairam V, Ramanibai R. 2018. Chitin and chitosan preparation from shrimp shells *Penaeus monodon* and its human ovarian cancer cell line, PA-1. Intl J Biol Macromol 107: 662-667. DOI: 10.1016/j.ijbiomac.2017.09.035.

Stefaniak J, Nowak MG, Wojciechowski M, Milewski S, Skwarecki AS. 2022. Inhibitors of glucosamine-6-phosphate synthase as potential antimicrobials or antidiabetics-synthesis and properties. J Enzyme Inhib Med Chem 37 (1): 1928-1956. DOI: 10.1080/14756366.2022.2096018.

Strzelecka M, Świątek P. 2021. 1,2,4-Triazoles as important antibacterial agents. Pharmaceuticals (Basel) 14 (3): 224. DOI: 10.3390/ph14030224.

Sumarto. 2020. Characteristics of Sand Sea Cucumber (*Holhuria scabra* J.) and Potential of Glucosamine Extract for Synovial Fluid Production in Osteoarthritis Patients. Universitas Riau, Pekanbaru. [Indonesian]

Suptijah P, Jacoeb AM, Rachmania D. 2011. Characterization chitosan nano from white shrimp shells (*Litopenaeus vannamei*) with ionic gelation methods. Indones J Fish Prod Proces 17 (2): 78-84. DOI: 10.17844/jphpi.v14i2.5315.

Suzuki N. 2021. Tissue N-Glycan Analysis Using LC-MS, MS/MS, and MS(n). current. Protocols e200: 1-48

Syukron F, Karnila R, Hasan B. Characteristics of Glucosamine Hydrochloride (HCl GlcN) from chitin and blue pond chitosan crab (*Portunus pelagicus*). Berkala Perikanan Terubuk 44 (2): 22-35. [Indonesian]

Tavares JO, Cotas J, Valado A, Pereira L. 2023. Algae food products as a healthcare solution. Mar Drugs 21 (11): 578. DOI: 10.3390/md21110578.

Taylor CJ, Pomberger A, Felton KC, Grainger R, Barecka M, Chamberlain TW, Bourne RA, Johnson CN, Lapkin AA. 2023. A brief introduction to chemical reaction optimization. Chem Rev 123 (6): 3089-3126. DOI: 10.1021/acs.chemrev.2c00798.

Teoh CF, Tuzan AD, Yong AS, Liew KS, Lim LS, Liew HJ. 2023. Evaluation of crystalline amino acid as potent stimulatory chemoattractants for the slipper lobster (*Thenus orientalis*). PeerJ 11: e15607. DOI: 10.7717/peerj.15607.

Thebiotek. 2024. Manufacturer and Supplier of High Quality Specialty Chemicals. Department RnD: California. https://www.thebiotek.com. [Accessed August 9, 2024]

Triunfo M, Tafi E, Guarnieri A, Salvia R, Scieuzo C, Hahn T, Zibek S, Gagliardini A, Panariello L, Coltelli MB, De Bonis A, Falabella P. 2022. Characterization of chitin and chitosan derived from *Hermetia illucens*, a further step in a circular economy process. Sci Rep 12: 6613. DOI: 10.1038/s41598-022-10423-5.

Vårum KM, Anthonsen MW, Grasdalen H, Smidsrød O. 1991. Determination of the degree of N-acetylation and the distribution of N-acetyl groups in partially N-deacetylated chitins (chitosans) by high-field n.m.r. spectroscopy. Carbohydr Res 211 (1): 17-23. DOI: 10.1016/0008-6215(91)84142-2.

Verardi A, Sangiorgio P, Lopresto CG, Casella P, Errico S. 2023. Enhancing carotenoids' efficacy by using chitosan-based delivery systems. Nutraceuticals 3 (3): 451-480. DOI: 10.3390/nutraceuticals3030033.

William W, Wid N. 2019. Comparison of extraction sequence on yield and physico-chemical characteristic of chitosan from shrimp shell waste. J Phys Conf Ser 1358: 012002. DOI: 10.1088/1742-6596/1358/1/012002.

Xu W, Kangxing Lv, Mu W, Zhou S, Yang Y. 2021a. Encapsulation of α-tocopherol in whey protein isolate/chitosan particles using oil-in-water emulsion with optimal stability and bioaccessibility. LWT 148: 111724. DOI: 10.1016/j.lwt.2021.111724.

Xu, Wang Y, Liu X, Zhang L, Jiang Q. 2021b. Chitosan from crab shell waste: A review on its preparation, characterization, and applications. Biol Macromol 166: 195-209.

Xue T, Wang W, Yang Z, Wang F, Yang L, Li J, Gan H, Gu R, Wu Z, Dou G, Meng Z. 2022. Accurate determination of the degree of deacetylation of chitosan using UPLC-MS/MS. Intl J Mol Sci 23 (15): 8810. DOI: 10.3390/ijms23158810.

Yuliasara F, Sari MN, Choriah MN, Mahmiah. 2019. Pembuatan kitin dan kitosan dari kulit udang vaname (*Litopenaeus vannamei*). Prosiding Seminakel 17: 102-108. [Indonesian]

Zhang Y, Xue C, Xue Y, Gao R, Zhang X. 2005. Determination of the degree of deacetylation of chitin and chitosan by X-ray powder diffraction. Carbohydr Res 340 (11): 1914-1917. DOI: 10.1016/j.carres.2005.05.005.

Zhang D, Bland JM, Xu D, Chung S. 2015. Degradation of chitin and chitosan by a recombinant chitinase derived from a virulent *Aeromonas hydrophila* isolated from diseased channel catfish. Adv Microbiol 5 (9): 611-619. DOI: 10.4236/aim.2015.59064.

Zhang J, Cheng X, Chang L, Zhang L, Zhang S. 2021. Combined treatments of chitosan and sodium silicate to inhibit *Alternaria alternata* pathogens of postharvest winter jujube. Food Sci Biotechnol 30 (4): 589-597. DOI: 10.1007/s10068-021-00890-3.

Zhang Z, Ma Z, Song L, Farag MA. 2024. Maximizing crustaceans (shrimp, crab, and lobster) by-products value for optimum valorization practices: A comparative review of their active ingredients, extraction, bioprocesses and applications. J Adv Res 57: 59-76. DOI: 10.1016/j.jare.2023.11.002.

Zhi-Hou L, Xiang G, Vincent CHC, Wen-Fang Z, Qi F, Yuebin L, Wang, Dong S, Xi-Ru Z, Peidong Z, Fu-Rong L, Qing-Mei H, Qing C, Wei-Qi S, Xian-Bo W, Xiaoming S, Virginia BK, Xingfen Y, Chen M. 2020. Associations of regular glucosamine use with all-cause and cause-specific mortality: A large prospective cohort study. Ann Rheum Dis 79 (6): 1-8. DOI: 10.1136/annrheumdis-2020-217176.

Zhou J, Wu Z, Lin Z, Wang W, Wan R, Liu T. 2022. Association between glucosamine use and cancer mortality: A large prospective cohort study. Front Nutr 9: 947818. DOI: 10.3389/fnut.2022.947818.